JOURNAL OF CATALYSIS 72, 294–302 (1981)

The Atomic Structure of Platinum Aggregates Encaged in Y Zeolite. Structure in the Course of Benzene Hydrogenation

P. GALLEZOT AND G. BERGERET

Institut de Recherches sur la Catalyse (CNRS), 2 avenue Albert Einstein, 69626 Villeurbanne Cédex, France

Received March 10, 1981; revised June 29, 1981

The atomic structure of 10-Å-diameter platinum aggregates encaged in Y-type zeolite has been studied by the radial electron distribution method from X-ray data. When the particles are free from adsorbates the structure is distorted and the interatomic distances are contracted with respect to the normal fcc structure of bulk platinum. On hydrogen adsorption the structure undergoes a total relaxation, and the aggregates exhibit the normal fcc structure and interatomic distances. Benzene adsorption produces a weak relaxation but the structure is still distorted and contracted because the benzene overlayer coordinates the surface atoms less efficiently than dissociated hydrogen. In the course of benzene hydrogenation at 300 K with $P_{H_2}/P_{C_6H_6} = 3$ the structure is intermediate between that of the particles covered with hydrogen and that of the particles covered with C_6H_6; both reactants are therefore adsorbed on the surface. The structure is similar when the reaction is carried out with an excess of benzene ($P_{H_2}/P_{C_6H_6} = 1$); in this case the surface remains partially covered with irreversibly adsorbed hydrogen which does not participate in the hydrogenation reaction.

INTRODUCTION

Knowledge of the atomic structure of catalyst surfaces during catalytic reactions is needed to improve the understanding of heterogeneous catalysis. The composition and structure of the surface under working conditions are controlled by the kinetics of the elementary steps of the reaction when the incoming reactants, the surface intermediates and the outgoing products are in equilibrium with each other. Studies of the atomic and electronic structures of working catalyst surfaces are very rare because most of the modern analytical tools of surface science cannot be used under reaction conditions. Moreover, few of them are capable of giving information on the surface structure of very small metal particles on supports. It has been shown that the radial electron distribution (RED) method (*1*) derived from X-ray diffraction data is well suited to the study of the effect of the adsorbates on the structure of metal aggregates where most of the atoms are on the surface (*2–4*). Thus it was shown that the 10-Å-diameter platinum particles encaged in Y zeolite have the normal fcc structure of bulk platinum when covered by dissociated hydrogen (*3*), whereas oxygen or sulfur adsorption leads essentially to disordered structures (*3, 4*). The aim of the present work is to study by the RED method the atomic structures of the same particles with a bare surface, after hydrogen or benzene adsorption, and in the course of the benzene hydrogenation reaction.

EXPERIMENTAL

1. Materials

The PtCeNaY zeolite was obtained from NaY Linde SK-40 sieve by successive ion exchanges firstly in water solutions of $Ce(NO_3)_3$ and secondly in ammonia solution of $PtCl_2$ as described previously (*5–7*). The unit cell composition of the dehydrated zeolite determined by the chemical analysis of Pt^{2+}, Ce^{3+}, and Na^+ cations was $Pt_{11}Ce_1Na_{19}H_{12}Y$ ($Y = Al_{56}Si_{136}O_{384}$). The zeolite (1-g batch) was activated in flowing O_2 up to 630 K at 0.5 K/min and reduced at

0021-9517/81/120294-09$02.00/0
Copyright © 1981 by Academic Press, Inc.
All rights of reproduction in any form reserved.

580 K under 400 Torr (1 Torr = 133.3 N m^{-2}) of hydrogen pressure. It was shown by high-resolution transmission electron microscopy on ultramicrotome cuts of the zeolite crystals that the sizes of platinum particles are in the range 7–11 Å. As noted previously (*7*), the presence of cerium even in a small amount favors the formation of smaller and more homogeneous particle sizes.

2. Procedure

The reduced zeolite was evacuated at 700 K for 16 h at 10^{-5} Torr. Then, in a glove box flushed with oxygen-free dry argon, the zeolite was transferred into an X-ray cell designed to record the X-ray diffraction pattern. The zeolite powder was pressed into a rectangular cavity drilled in the inside of the back of the X-ray cell. Benzene or hydrogen could be adsorbed on the zeolite while the X-ray cell was connected to a vacuum or gas line. The benzene hydrogenation reaction was carried out with the setup described in Fig. 1. The partial pressures of H_2 and C_6H_6 in the reaction feed were fixed by changing the composition and flow rate of the Ar + H_2 mixture while the flow of benzene was kept constant (4 mmole h^{-1}). The reactions were performed at 300 K during the 7 days which were needed to collect the X-ray-diffracted intensities. The products of the reaction were analyzed periodically by on-line gas chromatography. Table 1 gives the nomenclature and treatments of the samples investigated.

3. RED analysis

The X-ray diffraction patterns were recorded with a stabilized Philips diffractometer using a 2400-W tube with molybdenum anode (Mo $K\bar{\alpha}$ = 0.710 Å). The X-ray cell equipped with a 180° beryllium window was mounted on the θ shaft of the Norelco goniometer, and the diffraction patterns were taken by reflection on the pressed zeolite sample. The diffracted intensities were monochromatized with a diffracted beam monochromator (curved quartz crystal with a narrow passband) which eliminates most of the Compton scattering. The Compton intensity left at small Bragg angles is very weak compared to the overall diffracted intensity. The RED curves calculated from the intensities measured with this setup were checked to be similar to those obtained with a Zr-filtered beam from which the calculated Compton intensities have been subtracted, however, the electron density peaks were better resolved with the present arrangement. The diffracted intensities were collected from 1 to at least 130° (2θ) by scanning with 0.125 (2θ) steps. Data collection required about 7 days (10 min per step) to obtain good counting statistics over the whole range of Bragg angles. The intensities were corrected for polarization and set on an absolute scale (electron^2 units) by matching them at high Bragg angles to the calculated independent scattering. The RED functions were calculated by Fourier transformation of the scaled intensities as previously described (*3*).

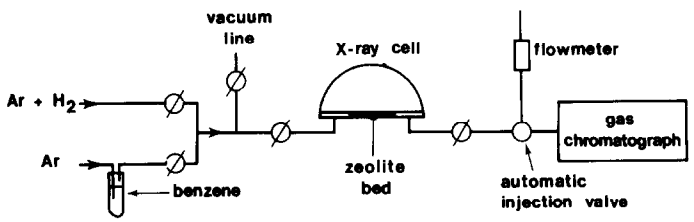

FIG. 1. Experimental arrangement designed to record the X-ray diffraction pattern in the course of benzene hydrogenation. The X-ray cell equipped with a 180° beryllium window is mounted on the shaft of the diffractometer.

TABLE 1

Nomenclature and Treatments of the $Pt_{11}Ce_1Na_{19}H_{12}Y$ Zeolite[a]

Sample	Treatments[b]	Atmosphere[c]
I. PtY (outgassed)	Activated at 630 K in O_2 Reduced at 580 K in H_2 (400 Torr) Evacuated at 700 K, 16 h, 10^{-5} Torr	Ar
II. PtY(C_6H_6)	Sample I contacted with 50 Torr of C_6H_6	Ar
III. PtY(H_2/C_6H_6 = 1)	Sample IV contacted with the reaction feed $P_{H_2}/P_{C_6H_6} = 1$	Reaction conditions
IV. PtY(H_2/C_6H_6 = 3)	Sample V contacted with the reaction feed $P_{H_2}/P_{C_6H_6} = 3$	Reaction conditions
V. PtY(H_2/C_6H_6 = 10^4)	Sample VI contacted with the reaction feed $P_{H_2}/P_{C_6H_6} = 10^4$	Reaction conditions
VI. PtY(H_2)	Sample I contacted with 100 Torr of H_2	Ar
VII. NaHY	$Na_{18}H_{38}Y$ dehydrated at 600 K under vacuum	Ar

[a] Containing 10-Å Pt particles.
[b] Temperatures of adsorption and reaction 300 K.
[c] Atmosphere in the X-ray cell during data recording (760 Torr).

RESULTS

The RED exhibits peaks at values of r corresponding to the interatomic distances in the scattering medium and the intensities of the peaks are proportional to the number of interatomic vectors (I). The RED of the platinum-free NaHY zeolite is given in Fig. 2 (curve 1). The best characterized peak at 1.65 Å corresponds to the weighted average of Al–O and Si–O distances while the shoulder at 2.65 Å and the broad peak at 3.15 Å correspond to O–O and (Si, Al)–(Si, Al) distances, respectively. At larger r values the distribution merges into a continuum of interatomic distances. This monotonic distribution is due to the complex arrangement of the zeolite framework involving about 600 atoms per unit cell. On the other hand the RED of sample PtY(H_2) (Fig. 2, curve 2) exhibits sharp and large electron density peaks which can all be attributed to the interatomic vectors appearing in the platinum fcc structure, since they correspond to the normal Pt–Pt distances of bulk platinum. Although the peaks corre-

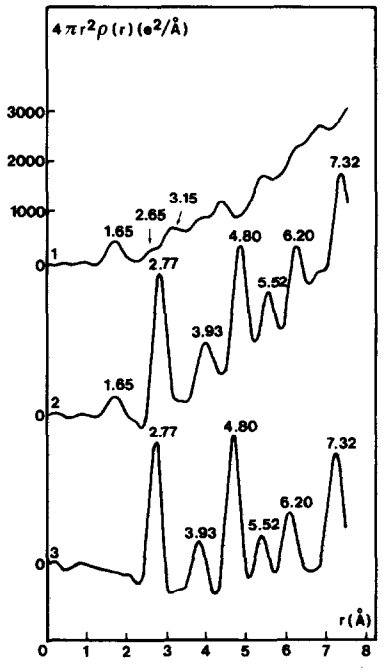

FIG. 2. Radial electron distributions. (1) RED of the platinum-free support (sample VII, NaHY); (2) RED of the platinum zeolite (sample VI, PtY(H_2)); (3) difference RED obtained by subtracting curve 1 from curve 2.

sponding to the atoms of the support are superimposed on this distribution they do not impede its interpretation. This is because they are much smaller than the Pt–Pt electron density peaks and therefore the RED of Pt zeolites could be used as such to study the structure of the platinum aggregates. However, a still better resolution of the Pt–Pt peaks was obtained by subtracting the RED of NaHY from the RED of PtY(H_2). The difference RED (Fig. 2, curve 3) no longer exhibits the 1.65-Å peak and the other peaks from the support atoms which decreased somewhat the resolution of the Pt–Pt peaks in curve 2; the interatomic distances are not appreciably modified. The difference procedure does not eliminate the interatomic vectors between the platinum atoms and the framework atoms. However, these vectors are expected to be quite random, and actually no peak other than the Pt–Pt peaks was observed on the difference distribution. The RED of NaHY was systematically subtracted from the RED of the PtY samples investigated, and the resulting support-free REDs are given in Fig. 3. The interatomic distances and the magnitudes of the Pt–Pt peaks are given in Table 2.

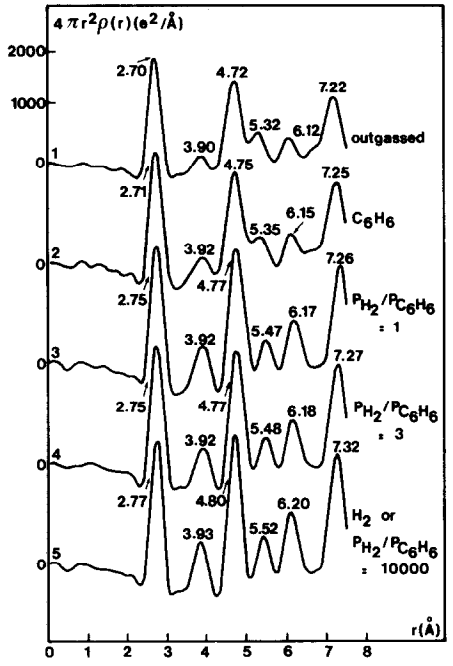

FIG. 3. Radial electron distributions of the 10-Å platinum particles obtained by subtracting the RED of the support. (1) RED of the bare particles (sample I); (2) RED of the particles covered with C_6H_6 (sample II); (3) RED of the particles during reaction, $P_{H_2}/P_{C_6H_6} = 1$ (sample III); (4) RED of the particles during reaction, $P_{H_2}/P_{C_6H_6} = 3$ (sample IV); (5) RED of the particles during reaction $P_{H_2}/P_{C_6H_6} = 10^4$ (sample V) or the particles covered with hydrogen (sample VI).

The benzene hydrogenation reaction was carried out successively with a large excess of hydrogen ($P_{H_2}/P_{C_6H_6} = 10^4$), with the stoichiometric mixture ($P_{H_2}/P_{C_6H_6} = 3$), and also with an excess of benzene ($P_{H_2}/P_{C_6H_6} = 1$). During the experiments, the conversion of benzene did not change from the first few minutes of reaction to the end of the X-ray pattern recording which took 7 days for each experiment. The apparent conversion was higher than 50% in the three reactions. Unfortunately the true conversion rate could not be measured because of the geometry of the X-ray cell and of the zeolite bed. Indeed, part of the reactant mixture could flow across the cell without contacting the zeolite, so the actual conversion of benzene interacting with the catalyst was probably 100% in every case.

DISCUSSION

1. Structure of the Bare Platinum Particles

As shown previously (*3*) the RED of the 10-Å Pt particles covered with hydrogen (PtY(H_2), Fig. 3, curve 5) exhibits all the Pt–Pt peaks corresponding to the successive coordination shells of the fcc structure with the interatomic distances of bulk platinum (Table 2). The RED of the same particles outgassed at 700 K and kept under argon (sample I in Fig. 3, curve 1) shows basically the same peaks. However, there are conspicuous differences: (i) all the distances are shorter than in PtY(H_2), but the contraction is uneven in that the distances at 2.77, 4.80, and 5.52 Å are now 2.5, 1.7, and 3.6% shorter, respectively; (ii) the

TABLE 2

Interatomic distances (Å) and Magnitudes of the Pt–Pt Peaks (e^2/Å)

Samples	Coordination spheres (nearest neighbours)						Percentage of relaxation[a]
	1st	2nd	3rd	4th	5th	7th	
I. PtY (outgassed)	2.70[b]	3.90	4.72	5.32	6.12	7.22	0
	2080[c]	140	1635	610	497	1296	0
II. PtY(C_6H_6)	2.71	3.92	4.75	5.35	6.15	7.25	27
	2191	140	1808	491	587	1583	27
III. PtY(H_2/C_6H_6 = 1)	2.75	3.92	4.77	5.47	6.17	7.28	64
	2340	340	2275	460	878	1959	73
IV. PtY(H_2/C_6H_6 = 3)	2.75	3.92	4.77	5.50	6.18	7.28	64
	2360	311	2257	526	871	1985	75
V. PtY(H_2/C_6H_6 = 10^4)	2.77	3.93	4.80	5.52	6.20	7.32	100
	2450	460	2587	566	1051	2220	100
VI. PtY(H_2)	2.77	3.93	4.80	5.52	6.20	7.32	100
	2440	460	2483	550	1082	2200	100
Distances in bulk Pt	2.774	3.923	4.805	5.548	6.203	7.339	

[a] The percentage of relaxation of the structure is estimated from the variations of the interatomic distances (first figure) and from the variations of the peak magnitudes (second figure). These values are calculated on the three major peaks (2.77, 4.80, and 7.32 Å).

[b] Interatomic distance (Å).

[c] Peak height (e^2/Å).

magnitudes of the peaks decrease faster with r than in PtY(H_2), the three major peaks at 2.70, 4.72, and 7.22 Å being 15, 37, and 42% smaller, respectively; (iii) the Pt–Pt peaks become slightly broader and their resolution decreases with r. These observations lead us to conclude that in addition to the contraction of the interatomic distances the structure of the bare particles is distorted with respect to the ordered fcc structure.

The contraction and distortion of the atom packing could be due to an intrinsic size effect. Indeed, when the sizes of metal aggregates decrease below 15 Å the fraction of surface atoms is rapidly increasing. Since the coordination of these atoms is incomplete one can expect modifications of the interatomic distances and of the atom packing. Calculations of the minimum energy configuration of clusters (*8, 9*) indicate that the atoms can significantly depart from their equilibrium position occupied in the fcc structure to gain a more favorable coordination by increasing the number of their nearest neighbours and by becoming closer to the underneath atoms in the core of the cluster. Ultimately the tangential and normal shifts of atoms can result in the building of a polytetrahedral or icosahedral structure (*10*) in which the coordination number of the surface atoms is increased (*11*). Actually the presence of such noncrystal structures (without long-range order) can neither be ruled out nor be confirmed because the RED of sample I is consistent either with a mixture of fcc particles and of noncrystal particles with contracted bond lengths or with contracted and distorted fcc particles. The calculation of RED from models and the comparison of calculated and experimental REDs would be inconclusive because there are too many parameters involved, viz., particle sizes (distribution 5 to 12 Å), particle shapes, bond length contraction, percentages of particles with the

fcc structure and with the noncrystal structure, and nature of the noncrystal structure (polytetrahedral or icosahedral). At any rate a sizable fraction of particles do have the fcc structure since polytetrahedral particles and small icosahedra would not exhibit any peak near 3.92 Å corresponding to atoms in square arrangement (100 facet).

From the above discussion it turns out that the distortion and the contraction of the structure of the bare 10-Å particles can be intrinsic, in agreement with the forecast of cluster calculations. However, these calculations do not take into account the particle environment. Actually the particles are encaged in the supercages of the zeolite in close vicinity with the 48 oxygen anions building the cage walls. We have shown previously (*7, 12*) that the electronic structure of the 10-Å platinum particles is modified by the environment involving the crystal field of the zeolite framework and of the cations and also the acidity of the zeolite. Indeed, modifications of the electronic structure and of the geometric structure of atoms are always associated (*11*); thus the electron-deficient character of the platinum in 10-Å aggregates which is mainly induced by a support effect might be associated with the contraction of bond lengths. At this point it is reasonable to suggest that the intrinsic size effect and the support effect are superimposed. Further experimental and theoretical investigations will be needed to find out which is the main effect responsible for the lattice contraction and distortion. We may note that the contraction of the first nearest-neighbours distance was also observed by EXAFS (*19*).

2. *Effects of the Hydrogen and Benzene Adsorptions*

From the data given in Table 2 and from the comparison of curves 1 (PtY (outgassed)) and 5 ($PtY(H_2)$) in Fig. 3 it emerges that the adsorption of hydrogen produces a total relaxation of the structure of the bare clusters toward the normal fcc structure. This reordering occurs because the surface platinum atoms are now covered by strongly bonded hydrogen atoms (the Pt–H binding energy derived from the experimental heats of chemisorption (*13*) and from the dissociation energy of H_2 is in the range 60–65 kcal · mole^{-1}). The surface atoms recover the fcc packing because their coordination is now completed by hydrogen. In a sense the adsorbed hydrogen atoms prolong the platinum cluster and the Pt atoms underneath the hydrogen layer are ordered like bulk atoms.

On the other hand the adsorption of benzene on the bare 10-Å particles (Fig. 3, curve 2) induces only a slight relaxation of the structure (the Pt–Pt distances increase by ca. 0.5% and the three major peaks recover 27% of their intensity (Table 2)). The structure under the layer of benzene is weakly perturbed because there is a weak interaction between the C_6H_6 molecules and the surface platinum atoms. Indeed the heats of benzene chemisorption on metals reported in the literature have low values (e.g., 12 kcal · mole^{-1} on nickel (*14*)); furthermore, since at least six metal atoms are involved in accommodating a single C_6H_6 molecule the binding energy of the molecule per surface atom is at least six times weaker. The structure of the particles covered with benzene therefore remains contracted and distorted because the surface atoms remain coordinatively unsaturated. These results make for an associative adsorption mechanism since a dissociative benzene chemisorption would spill hydrogen atoms on the platinum surface thereby producing a larger relaxation of the structure.

The preceding interpretation of the weak structure relaxation in terms of the weak benzene–platinum interaction could be questioned in view of the incomplete accessibility of the encaged Pt particles. If we consider the particles filling entirely the volume of the supercages the C_6H_6 molecules can only interact with the fraction of the surface facing the four 7.5-Å-diameter

apertures. In the hypothesis where the distortion of the structure is due to the crystal field of the zeolite (see Section 1) one could argue that the distortion persists after benzene adsorption because the surface of the particle facing the cage walls remains unshielded. In the hypothesis of an intrinsic distortion (see Section 1) one could also argue that the distortion persists because part of the surface remains uncovered with benzene. Whatever the hypothesis hydrogen would produce a large relaxation since all the atoms are accessible to hydrogen atoms, as shown previously (*5*). However, we do not believe that the accessibility question can challenge our preceding interpretation because (i) about half the surface of the particle filling the supercages is accessible at the four supercage apertures, (ii) a number of particles detected by electron microscopy are small enough (<8 Å) to let the benzene molecules enter the cages. Furthermore, there is experimental evidence (*15, 16*) showing the presence in the supercages of PtY zeolites of particles smaller than those which can be detected by electron microscopy (<5–6 Å).

3. Effect of Benzene Hydrogenation

During benzene hydrogenation on the platinum zeolite the structure of the metal surface can change locally (on the atomic scale) and periodically (e.g., according to the site time yield). However, since the X-ray intensities are diffracted by all the atoms in the solid and over a long period of time the RED calculated from these intensities gives a space- and time-averaged structure. We have checked that the RED does not change in successive data recordings with the same reaction conditions and therefore the average structure is stable on the time scale of our experiments.

When the zeolite previously outgassed or covered with hydrogen is contacted with a reactant flow containing a large excess of hydrogen ($P_{H_2}/P_{C_6H_6} = 10^4$) the RED is similar to that of the zeolite covered with H_2 (sample V, Fig. 3, curve 5). This indicates that almost all the platinum atoms are covered with hydrogen and the particles exhibit the normal fcc structure. This result is not surprising, taking into account the reaction conditions [2 mmole h^{-1} of benzene (half the total flow because of the geometry of the X-ray cell), turnover frequency of 80 h^{-1} at 25°C (*5*), 0.15 g of 100% dispersed Pt present in the zeolite bed], so about 3% of the total platinum surface is needed to convert totally the benzene contacting the zeolite bed. Therefore the benzene is adsorbed and converted into cyclohexane in the upper layer of the zeolite bed, i.e., on a negligible fraction of the surface, leaving the main fraction covered by hydrogen.

When the reactant flow contains a stoichiometric mixture of hydrogen and benzene ($P_{H_2}/P_{C_6H_6} = 3$) the RED (sample IV, Fig. 3, curve 4) shows that the interatomic distances, as well as the magnitude and the resolution of the Pt–Pt peaks, are intermediate between those observed for the zeolite covered with benzene (curve 2) and those covered with hydrogen (curve 5). Table 2 indicates that the percentage of relaxation with respect to the outgassed structure is 75%, whereas the relaxation in the case of benzene adsorption was only 27% (see Section 2). It can be concluded that under these reaction conditions the space- and time-averaged structure corresponds to particles covered both with adsorbed benzene molecules and with adsorbed hydrogen atoms. This is consistent with a Langmuir–Hinshelwood mechanism where the molecules react in the adsorbed state. However, the present results do not prove that all the molecules and atoms adsorbed on the surface participate in the reaction. Indeed, when the flow of reactants contains an excess of benzene ($P_{H_2}/P_{C_6H_6} = 1$), the RED (sample III, Fig. 3, curve 3) is quite similar to that observed with the stoichiometric mixture (curve 4). This indicates that the structure of the particles is exactly the same and therefore that the surface remains covered with the same fraction of hydrogen and with the same fraction of

benzene as those previously, although one might have expected an overwhelming benzene coverage. One is led to conclude that a large fraction of the surface is occupied by irreversibly adsorbed hydrogen atoms, i.e., by atoms which are not displaced by benzene and which are unavailable to hydrogenate the benzene molecules. This is in agreement with previous experiments on Pt/Al_2O_3 showing by infrared spectroscopy (*17*) that there is no catalytic hydrogenation when the benzene is adsorbed on a surface covered with irreversibly adsorbed hydrogen. Also magnetic measurements on Raney nickel (*18*) showing that benzene adsorption takes place on a smaller number of Ni atoms in the presence of preadsorbed hydrogen than without hydrogen indicate that part of the hydrogen is not displaced by benzene.

CONCLUSIONS

This investigation and the previous ones (*2–4*) show that the RED method derived from X-ray diffraction measurements is a valuable tool to study the structure of supported metal aggregates. It should be stressed again that the accuracy of the structural information obtained by this method depends upon the magnitude of the metal scattering factor, upon the metal concentration, and upon the nature and structure of the support. The Y zeolite loaded with 15 wt% of platinum is of course a choice material to obtain the best contrast between the RED peaks corresponding to the interatomic vectors of the metal and those of the support. Moreover, since the platinum is 100% dispersed in the zeolite pores the structure of the aggregates is highly sensitive to the environment and especially to the molecules and atoms adsorbed on their surface.

It was shown that when the surface of the 10-Å Pt aggregates is free from adsorbates their structure is contracted and distorted with respect to the normal fcc structure of platinum. The adsorption of hydrogen produces a total relaxation of the structure of the bare particles toward the ordered fcc packing and the interatomic distances of bulk metal, whereas benzene adsorption produces only a weak relaxation of the structure. These differences are related to the different nature of the surface complexes formed between the Pt atoms and the hydrogen atoms on the one hand and between the Pt atoms and the benzene molecules on the other. It appears that the hydrogen atom ligands fulfill the coordination of the surface atoms much better than the benzene molecules. This is because each Pt atom can be coordinated directly by at least one hydrogen atom with a large binding energy whereas the linkage of the benzene molecule to the surface is energetically much weaker. On the other hand, adsorbed oxygen or sulfur atoms interact so strongly with the platinum atoms that they lead to disordered structures with a beginning of structure reconstruction as evidenced by the formation of Pt–O–Pt and Pt–S–Pt linkages (*3, 4*). Clearly the structure of the metal aggregates cannot be regarded as definitively fixed since the adsorbates can lead to various rearrangements of the atoms from weak relaxations to total structure reconstructions.

This investigation was the first attempt to determine the structure of metal aggregates in the course of a catalytic reaction. The conclusion that the surface is covered both by adsorbed benzene and by adsorbed hydrogen during the hydrogenation of benzene was expected because this is in agreement with all the proposed reaction mechanisms of the Langmuir–Hinshelwood type. Less expected was the fact that benzene covers only a fraction of the metal surface which does not change even in the presence of a large excess of benzene in the gas phase. This result is in agreement with a zero reaction order since the coverage in benzene does not depend on pressure, but the important corollary is that a large fraction of the surface remains covered by irreversibly adsorbed hydrogen which is not displaced by benzene and which does not

participate in the reaction. Further investigations with $P_{H_2}/P_{C_6H_6}$ ratios larger than 3 (but much smaller than 10^4) should be carried out to study the variance of the surface composition and to check if part of the surface is also covered by irreversibly adsorbed benzene.

REFERENCES

1. Ratnasamy, P., and Leonard, A. J., *Catal. Rev. Sci. Eng.* **6**, 293 (1972).
2. Ratnasamy, P., Leonard, A. J., Rodrigue, L., and Fripiat, J. J., *J. Catal.* **29**, 374 (1973).
3. Gallezot, P., Bienenstock, A., and Boudart, M., *Nouv. J. Chim.* **2**, 263 (1978).
4. Gallezot, P., *in* "Proceedings, 5th Int. Conf. Zeolites" (L. V. C. Rees, Ed.), p. 364. Heyden, London, 1980.
5. Gallezot, P., Alarcon-Diaz, A., Dalmon, J. A., Renouprez, A. J., and Imelik, B., *J. Catal.* **39**, 334 (1975).
6. Gallezot, P., Datka, J., Massardier, J., Primet, M., and Imelik, B., *in* "Proceedings, 6th International Congress on Catalysis, London, 1976" (G. C. Bonds, P. B. Wells, and F. C. Tompkins, Eds.), Vol. 2, p. 696. The Chemical Society, London, 1977.
7. Tri, T. M., Massardier, J., Gallezot, P., and Imelik, B., *in* "Proceedings 7th International Congress on Catalysis, Tokyo, 1980," p. 266. Elsevier, Amsterdam, 1981.
8. Burton, J. J., *Nature* **229**, 335 (1971).
9. Hoare, M. R., and Pal, P. J., *Cryst. Growth* **17**, 77 (1972).
10. Burton, J. J., *Catal. Rev. Sci. Eng.* **9**, 209 (1974).
11. Gordon, M. B., Cyrot-Lackmann, F., and Desjonquères, M. C., *Surf. Sci.* **68**, 359 (1977).
12. Gallezot, P., Weber, R., Dalla Betta, R. A., and Boudart, M., *Z. Naturforsch. A* **34**, 40 (1979).
13. Toyoshima, I., and Somorjai, G. A., *Catal. Rev. Sci. Eng.* **19**, 105 (1979).
14. Babernics, C., and Tétényi, P., *J. Catal.* **17**, 35 (1970).
15. Dalla Betta, R. A., and Boudart, M., *J. Chem. Soc. Faraday Trans. I* **72**, 1723 (1976).
16. de Menorval, L. C., Ito, T., and Fraissard, J. P., *J. Phys. Chem.*, in press.
17. Basset, J. M., Dalmai-Imelik, G., Primet, M., and Mutin, R., *J. Catal.* **37**, 22 (1975).
18. Candy, J. P., Dalmon, J. A., Fouilloux, P., and Martin, G. A., *J. Chim. Phys.* **72**, 1075 (1975).
19. Moraweck, B., Clugnet, G., and Renouprez, A. J., *Surf. Sci.* **81**, 1631 (1978).